THE FASEB JOURNAL • RESEARCH • www.fasebj.org

Intranasal administration of mesenchymoangioblast-derived mesenchymal stem cells abrogates airway fibrosis and airway hyperresponsiveness associated with chronic allergic airways disease

Simon G. Royce,*,†,1 Siddharth Rele,* Brad R. S. Broughton,‡ Kilian Kelly,§ and Chrishan S. Samuel*,2

*Fibrosis Laboratory and ‡Cardiovascular and Pulmonary Pharmacology Group, Cardiovascular Disease Program, Biomedicine Discovery Institute and Department of Pharmacology, Monash University, Clayton, Victoria, Australia; †Department of Medicine, Central Clinical School, Monash University, Prahran, Victoria, Australia; and §Cynata Therapeutics, Armadale, Victoria, Australia

ABSTRACT: Structural changes known as airway remodeling (AWR) characterize chronic/severe asthma and contribute to lung dysfunction. Thus, we assessed the *in vivo* efficacy of induced pluripotent stem cell and mesenchymoangioblast-derived mesenchymal stem cells (MCA-MSCs) on AWR in a murine model of chronic allergic airways disease (AAD)/asthma. Female Balb/c mice were subjected to a 9-wk model of ovalbumin (Ova)-induced chronic AAD and treated intravenously or intranasally with MCA-MSCs from weeks 9 to 11. Changes in airway inflammation (AI), AWR, and airway hyperresponsiveness (AHR) were assessed. Ova-injured mice presented with AI, goblet cell metaplasia, epithelial thickening, increased airway TGF-β1 levels, subepithelial myofibroblast and collagen accumulation, total lung collagen concentration, and AHR (all $P < 0.001$ *vs.* uninjured control group). Apart from epithelial thickness, all other parameters measured were significantly, although not totally, decreased by intravenous delivery of MCA-MSCs to Ova-injured mice. In comparison, intranasal delivery of MCA-MSCs to Ova-injured mice significantly decreased all parameters measured (all $P < 0.05$ *vs.* Ova group) and, most notably, normalized aberrant airway TGF-β1 levels, airway/lung fibrosis, and AHR to values measured in uninjured animals. MCA-MSCs also increased collagen-degrading gelatinase levels. Hence, direct delivery of MCA-MSCs offers great therapeutic benefit for the AWR and AHR associated with chronic AAD.—Royce, S. G., Rele, S., Broughton, B. R. S., Kelly, K., Samuel, C. S. Intranasal administration of mesenchymoangioblast-derived mesenchymal stem cells abrogates airway fibrosis and airway hyperresponsiveness associated with chronic allergic airways disease. FASEB J. 31, 4168–4178 (2017). www.fasebj.org

KEY WORDS: asthma · airway remodeling · therapies · pulmonary delivery

Asthma is a chronic respiratory disease affecting ~300 million people worldwide and is attributed to 250,000 annual deaths (1). There are 3 main components to its pathogenesis: airway inflammation (AI); airway remodeling (AWR), which represents structural changes in the airways/lung that eventually lead to airway fibrosis and obstruction; and airway hyperresponsiveness (AHR), which is the clinical feature of asthma. AWR can result from persistent or chronic AI but can also develop and contribute to AHR independently of AI (2, 3).

Current asthma therapy, including corticosteroids and β-agonists, is focused on symptom management rather than disease regression and is therefore not fully effective (4). Individuals treated with β-agonist–based therapies have relief of their asthma symptoms, but their underlying AI persists. As such, individuals requiring chronic use of β-agonists are at a greater risk of serious worsening of asthma, leading to hospitalization and death (5, 6). The gold-standard therapy of corticosteroids is also ineffective in treating the severe and severe-refractory subpopulations of patients with asthma. Patients with severe asthma often need treatment with high doses of corticosteroids that can be associated with systemic side effects (7) and do not necessarily improve lung function or quality of life (8, 9). Additionally, the severe refractory subgroup of patients

ABBREVIATIONS: AAD, allergic airways disease; ABPAS, Alcian blue periodic acid Schiff; AHR, airway hyperresponsiveness; AI, airway inflammation; AWR, airway remodeling; α-SMA, α-smooth muscle actin; BM, basement membrane; ECM, extracellular matrix; IHC, immunohistochemistry; IN, intranasal; iPSC, induced pluripotent stem cell; IV, intravenous; MCA, mesenchymoangioblast; MMP, matrix metalloproteinase; MSC, mesenchymal stem cell; Ova, ovalbumin; Sal, saline

[1] Correspondence: Fibrosis Laboratory, Department of Pharmacology, Monash University, Clayton, VIC 3800, Australia. E-mail: simon.royce@monash.edu

[2] Correspondence: Fibrosis Laboratory, Department of Pharmacology, Monash University, Clayton, VIC 3800, Australia. E-mail: chrishan.samuel@monash.edu

doi: 10.1096/fj.201700178R

0892-6638/17/0031-4168 © FASEB

with asthma shows fixed airway restriction (7), and therefore this population displays the critical role of AWR as part of their asthma symptoms, highlighting an urgent need for treatment strategies that can target and reduce AWR.

Mesenchymal stem cells (MSCs) are multipotent stromal cells that have the capacity to divide into a number of cell lineages. These cells express class I major histocompatibility complex but lack class II major histocompatibility complex and costimulatory molecules CD80, CD86, and CD40 (10, 11) and hence are immunoprivileged. As such, MSCs can be administered systemically *via* intravenous (IV) infusion, allowing for a broad distribution (12). Upon administration, MSCs accumulate in the lung (13). MSCs also home to the injured tissue through the expression of the chemokine receptor type 4, and the expression of this receptor is heightened in a proinflammatory environment such as in asthma, enhancing their homing ability (14). MSCs can also be administered directly into the lungs *via* intranasal (IN) instillation (15) and *via* the intratracheal route (12, 16).

Murine models of allergic airways disease (AAD), which mimic several features of human asthma, have been used to show that MSCs exhibit immunomodulatory (17) and anti-inflammatory (18) properties through both direct cell-cell contact and the secretion of paracrine factors. Administration of exogenous MSCs was shown to decrease Th2 proliferation and reduce Th2 bias, which contributes to AAD (18, 19). Suppression of dendritic cell activation, migration, and antigen presentation has been observed (20), and a decrease in eosinophil-associated proinflammatory cytokines was observed in bronchoalveolar lavage fluid (18). Compared with corticosteroids, which suppress AI, MSCs have been shown in these models to actively reduce the presence and activity of the cells responsible for inflammation.

Furthermore, MSC treatment has been shown to reduce epithelial thickness, smooth muscle hyperplasia, and goblet cell metaplasia in the airways (21). MSCs modestly decrease subepithelial and total collagen deposition (fibrosis) through their ability to promote collagen-degrading gelatinase levels (15), suggesting that MSCs also have antiremodeling actions. However, MSCs have not consistently demonstrated the ability to relieve the adverse symptoms associated with chronic disease settings, and the outcomes of MSC treatment can vary depending on their tissue origin/source, extent of culture expansion, donor-dependent viability and efficacy, and the timing of their administration (3, 22–24). This has likely contributed to the slow progression toward the clinical utility of MSCs from various sources for their therapeutic and tissue-reparative functions (25). Additionally, because only a relatively small number of MSCs can be isolated from each donor organ, a continuous supply of donors would be needed to facilitate sufficient numbers for experimental and commercial use.

To overcome these limitations, Cynata Therapeutics have used Cymerus technology to differentiate human induced pluripotent stem cells (iPSCs) into precursor cells known as mesenchymoangioblasts (MCAs; a class of early clonal mesoendodermal precursor cells) and subsequently into mesenchymal stem cells (MCA-MSCs) (26). Because iPSCs can proliferate indefinitely and because MCAs can expand into extremely large quantities of MSCs, sufficient MCA-MSCs can be acquired from a single master cell bank of iPSCs derived from a single healthy blood donor (limiting donor- and expansion-dependent variability and contamination from nontarget cells) without the need for excessive culture expansion once MSCs are formed. In this study, we investigated the therapeutic potential of these MCA-MSCs when delivered to a well-established murine model of chronic AAD, which presents with the 3 central features of human asthma: AI, AWR, and AHR (15, 27). In particular, we compared the antiremodeling effects of IV *vs.* IN administration of MCA-MSCs in the model used.

MATERIALS AND METHODS

Animals

Female Balb/c mice (6–8 wk old) were obtained from Monash Animal Services (Monash University, Clayton, VIC, Australia) and housed under a controlled environment on a 12-h light/12-h dark cycle with free access to water and lab chow (Barastock Stockfeeds, Pakenham, VIC, Australia). All mice were provided an acclimatization period of 4–5 d before experimentation, and all procedures performed were approved by a Monash University Animal Ethics Committee (MARP/2016/078) and complied with the *Guidelines for the Care and Use of Laboratory Animals for Scientific Purposes* (National Health and Medical Research Council, Canberra, ACT, Australia).

Induction of chronic AAD

To assess the effects of MSCs in chronic AAD, an ovalbumin (Ova)-induced model of chronic AAD was established in mice ($n = 24$). Mice were sensitized with 2 intraperitoneal injections of 10 μg grade V chicken egg Ova (Sigma-Aldrich, St. Louis, MO, USA) and 400 μg of aluminum potassium sulfate adjuvant (alum; Ajax Chemicals, Auburn, NSW, Australia) on d 0 and 14. They were then challenged by whole-body inhalation exposure (nebulization) to aerosolized Ova [2.5% w/v in 0.9% normal saline (Sal)] for 30 min, 3 times a week, between d 21 and 63, using an ultrasonic nebulizer (NE-U07; Omron, Kyoto, Japan). Control mice ($n = 24$) were given intraperitoneal injections of 500 μl 0.9% Sal instead of Ova and nebulized with 0.9% Sal.

MCA-MSC treatment

Twenty-four hours after the establishment of chronic AAD (on d 64), subgroups of Ova- or Sal-sensitized/challenged mice ($n = 8$ mice/group) underwent IV or IN administration of MCA-MSCs. In all cases, a 14-d treatment period (from d 64 to 77) was chosen to replicate the time frame used to evaluate the intranasally delivered effects of other stem cells, such as human bone marrow–derived (stromal) MSCs (15, 28) and human amnion epithelial cells (28), in the Ova-induced chronic model of AAD.

MCA-MSCs, which were produced from a clinical-grade iPSC line in chemically defined and serum-free conditions, were provided by Cynata Therapeutics (Armadale, VIC, Australia). A defining characteristic of MSCs is expression of CD73, -90, and -105 (29). MCA-MSCs were >99% positive for all 3 of these markers but were negative for CD43/45 and CD31, confirming the absence of hematopoietic and endothelial lineage cells. All treatments were administered once per week over the treatment period (on d 64 and 71). On the morning of each scheduled

treatment, frozen MCA-MSCs were thawed in a 37°C water bath and then resuspended as follows. For IV administration of MCA-MSCs, 1×10^7 cells were resuspended in 2 ml PBS. Mice were restrained in a Perspex restrainer (Perspex Distribution, Chelmsford, United Kingdom), and 1×10^6 cells/200 μl PBS were injected into the tail vein of Sal- or Ova-sensitized/challenged mice, which is a commonly used cell concentration delivered to mice (13, 15, 20, 28). For IN administration of MCA-MSCs, 1×10^7 cells were resuspended in 0.5 ml of PBS. Mice were lightly anesthetized with isoflurane (Baxter Health Care, Old Toongabbie, NSW, Australia) and held in a semisupine position while IN instillation took place. PBS (1×10^6 cells/50 μl) was then administered to the mice (25 μl per nare intranasally using an automatic pipette).

Invasive plethysmography

On d 78 (7 d after the last treatment of MCA-MSCs), mice were anesthetized with ketamine (10 mg/kg body weight) and xylazine (2 mg/kg body weight) in 0.9% Sal. Tracheostomy was performed on all mice with an 18-gauge tracheostomy tube. Mice were then placed in the chamber of the FinePointe Plethysmograph (Buxco Research Systems, Wilmington, NC, USA) and ventilated. Airway resistance of each mouse was measured in response to increasing doses of nebulized methacholine (Sigma-Aldrich) dissolved in PBS and delivered intratracheally from 6.25 to 50 mg/ml over 4 doses to elicit bronchoconstriction and evaluate AHR. The change in airway resistance (the maximum airway resistance after each dose minus the baseline resistance to PBS alone) was plotted against the corresponding dose of methacholine.

Tissue collection

After invasive plethysmography, lung tissues from each animal were isolated and rinsed in cold PBS before being divided into 4 separate lobes. The largest lobe was fixed in 10% neutral buffered formaldehyde overnight and processed to be cut and embedded in paraffin wax (for histologic and immunohistochemical analysis of various end-points). The remaining 3 lobes were snap-frozen in liquid nitrogen for various other assays.

Lung histopathology

Once the largest lobe from each mouse was paraffin embedded, each tissue block was serially sectioned (3 μm thickness) and placed on charged Mikro Glass slides (Grale Scientific, Ringwood, VIC, Australia) and subjected to various histologic stains or immunohistochemistry. For assessment of inflammation score, epithelial thickness, and subepithelial extracellular matrix (ECM) deposition, one section per slide from each mouse underwent Masson's trichrome staining. For assessment of goblet cell metaplasia, a second set of slides underwent Alcian blue periodic acid Schiff (ABPAS) staining. The Masson trichrome–stained and ABPAS-stained sections were morphometrically analyzed as detailed below.

Immunohistochemistry

Immunohistochemistry (IHC) was used to detect TGF-β1 (using a polyclonal antibody, sc-146, 1:1000 dilution; Santa Cruz Biotechnology, Santa Cruz, CA, USA) or α-smooth muscle actin (α-SMA), which is a marker of myofibroblast differentiation, using a mAb (M0851, 1:200 dilution; Dako, Glostrup, Denmark). Primary antibody staining was detected using the Dako EnVision anti-rabbit or anti-mouse kits and 3,3′-diaminobenzidine (DAB) chromogen. Negative controls, which were exposed to the EnVision kits in the absence of any primary antibody, were also included. All slides were then counterstained with hematoxylin and scanned by Monash Histology Services using ScanScope AT Turbo (Aperio, Sausalito, CA, USA) for morphometric analysis.

Morphometric analysis

Slides stained with Masson's trichrome, ABPAS, and IHC underwent morphometric analysis as follows. Five airways (of 150–300 μm in diameter) per section were randomly selected and analyzed using ImageScope software (Aperio). Masson's trichrome–stained slides underwent semiquantitative peribronchiolar inflammation scoring, where the experimenter was blinded and scored individual airways from 0 (no detectable inflammation surrounding the airway) to 4 (widespread and massive inflammatory cell aggregates, pooled size ~0.6 mm^2), as previously described (15). Masson's trichrome–stained slides also underwent analysis for epithelial thickness and subepithelial ECM deposition by measuring the thickness of the epithelium and the subepithelial ECM layer (stained blue), which were expressed as square micrometers per micrometer of basement membrane (BM) length.

Slides stained with ABPAS and α-SMA were analyzed for goblet cell metaplasia and subepithelial myofibroblast number, respectively, by counting the number of positively stained goblet cells or α-SMA–positive cells per 100 μm of BM length. TGF-β1–stained slides were analyzed for TGF-β1 protein expression by running an algorithm to assess strong positively stained pixels within the airway. Results were expressed as the number of strong positive pixels per total area (mm^2) of airway and then relative to that of the Sal-treated control group, which was expressed as 1.

Hydroxyproline assay

The second largest lung lobe from each mouse was processed as described before for the measurement of hydroxyproline content (15, 27), which was determined from a standard curve of purified *trans*-4-hydroxy-L-proline (Sigma-Aldrich). Hydroxyproline values were multiplied by a factor of 6.94, based on hydroxyproline representing ~14.4% of the amino acid composition of collagen in most mammalian tissues (30), to extrapolate total collagen content, which in turn was divided by the dry weight of each corresponding tissue to yield percent collagen concentration.

Gelatin zymography

The third largest lung lobe from each mouse was processed as detailed previously for extraction of proteins containing matrix metalloproteinases (MMPs) (31), and equal aliquots of total protein (10 μg/sample) were assessed on 7.5% acrylamide gels containing 1 mg/ml gelatin (15). Gelatinolytic activity was visualized as clear bands. Densitometry of MMP-9, which is the predominant gelatinase in the lung of female Balb/c mice (15), was performed using a GS710 Densitometer (Bio-Rad Laboratories, Gladesville, NSW, Australia) and Quantity-One software (Bio-Rad). The relative mean ± SEM optical density of MMP-9 was then graphed.

Statistical analysis

All statistical analysis was performed using Prism v6.0 (GraphPad Software, La Jolla, CA, USA) and expressed as means ± SEM.

AHR results were analyzed by 2-way ANOVA with Bonferroni *post hoc* test. The remaining data were analyzed by 1-way ANOVA with Neuman-Keuls *post hoc* test for multiple comparisons between groups. In each case, data were considered significant at $P < 0.05$.

RESULTS

Effects of MCA-MSCs on AI

AI was semiquantitated from hematoxylin and eosin–stained lung sections using an inflammation scoring system (from 0 to 4). The peribronchial inflammatory score of Ova-injured mice (2.75 ± 0.09) was significantly higher than that scored for the Sal-sensitized/challenged control mice (0.25 ± 0.09; $P < 0.001$ *vs.* Sal group) (**Fig. 1**). The elevated level of inflammation in the Ova group confirmed that these mice had been successfully sensitized and challenged with Ova.

IV administration of MCA-MSCs significantly reduced the Ova-induced peribronchial inflammatory cell infiltration (1.25 ± 0.23; $P < 0.001$ *vs.* Ova group) without affecting basal inflammation score when administered to Sal-treated control mice (Fig. 1). In comparison, IN administration of MCA-MSCs to Ova-injured mice induced a trend toward further lowering peribronchial inflammation (0.88 ± 0.13; $P < 0.001$ *vs.* Ova group) in the absence of any effects on inflammation in Sal-treated control mice (Fig. 1). However, neither treatment route of MCA-MSCs was able to fully reduce AI back to that measured in Sal-treated control mice ($P < 0.001$ *vs.* Sal group for IV treatment of MCA-MSCs to Ova-injured mice; $P < 0.05$ *vs.* Sal group for IN treatment of MCA-MSCs to Ova-injured mice).

Effects of MCA-MSCs on AWR

Goblet cell metaplasia

Goblet cell metaplasia was morphometrically assessed from ABPAS-stained lung sections and expressed as number of goblet cells per 100 μm of BM length (**Fig. 2**). Ova-treated mice had significantly increased goblet cell numbers (6.08 ± 0.52) compared with their Sal-treated control counterparts (0.001 ± 0.00; $P < 0.001$ *vs.* Sal group) (Fig. 2). Both IV (3.97 ± 0.64) and IN (2.89 ± 0.48) routes of administration of MCA-MSCs were able to significantly, although not totally, reduce the Ova-induced promotion of goblet cell numbers (both $P < 0.01$ *vs.* Ova group) (Fig. 2). Although neither route of MCA-MSC delivery restored the Ova-induced goblet cell metaplasia to that measured in Sal-treated control mice (both $P < 0.001$ *vs.* Sal group), MCA-MSCs did not affect goblet cell numbers in Sal-treated mice.

Airway epithelial thickness

Airway epithelial thickness was morphometrically assessed from Masson's trichrome–stained lung sections and expressed as square micrometers per micrometer of BM length (**Fig. 3**). The epithelial thickness of Ova-treated mice (19.16 ± 0.63 $\mu m^2/\mu m$) was significantly higher than that measured in Sal-treated control mice (14.28 ± 0.45 $\mu m^2/\mu m$; $P < 0.001$ *vs.* Sal group) (Fig. 3*A*, *B*). Whereas IV administration of MCA-MSCs did not affect the Ova-induced increase in epithelial thickness (18.59 ± 0.77 $\mu m^2/\mu m$), IN delivery of MCA-MSCs significantly, although not totally, decreased the thickness of the epithelium (16.67 ± 0.87 $\mu m^2/\mu m$) from that measured in the Ova group ($P < 0.05$ *vs.* Ova group; $P < 0.05$ *vs.* Sal group)

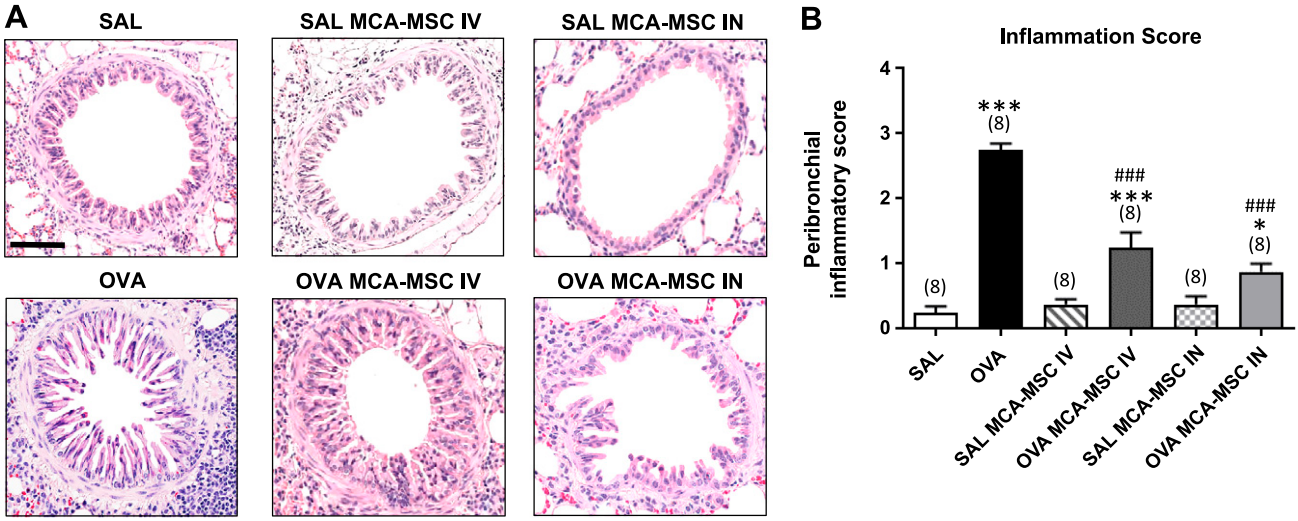

Figure 1. Effects of MCA-MSCs on peribronchial inflammation score. *A*) Representative photomicrographs of hematoxylin and eosin–stained lung sections from each of the groups studied show the extent of bronchial wall inflammatory cell infiltration present within and around the airway epithelial layer. Scale bar, 50 μm. *B*) Mean ± SEM inflammation score from 5 airways/mouse ($n = 8$ mice/group). Sections were scored for the number and distribution of inflammatory aggregates on a scale of 0 (no apparent inflammation) to 4 (severe inflammation). $^{*}P < 0.05$, $^{***}P < 0.001$ *vs.* Sal group; $^{\#\#\#}P < 0.001$ *vs.* Ova group.

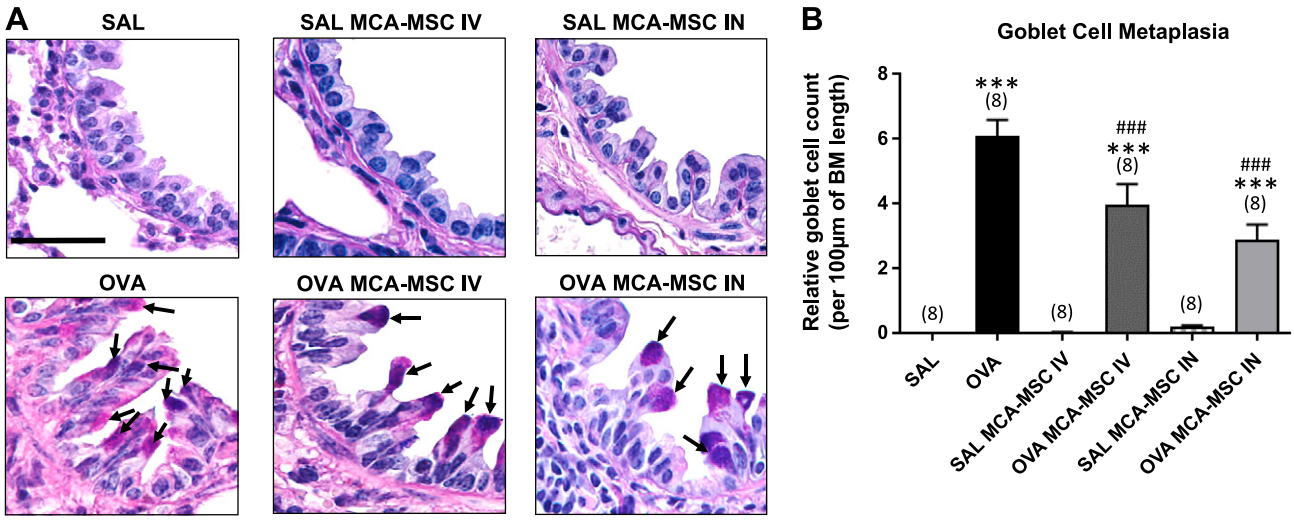

Figure 2. Effects of MCA-MSCs on goblet cell metaplasia. *A*) Representative photomicrographs of ABPAS-stained lung sections from each of the groups studied show the extent of goblet cells (indicated by arrows in Ova-injured mice only) within the airway epithelial layer. Scale bar, 25 µm. *B*) Goblet cell count from 5 airways/mouse (mean ± SEM; $n = 8$ mice/group). $^{***}P < 0.001$ *vs.* Sal group; $^{\#\#}P < 0.01$, $^{\#\#\#}P < 0.001$ *vs.* Ova group.

(Fig. 3*A*, *B*). The direct delivery of MCA-MSCs into the lungs *via* the IN route was also seen to offer greater protection against the Ova-induced increase in epithelial thickness compared with IV delivery of these cells [$P < 0.05$ *vs.* Ova MCA-MSC IV group] (Fig. 3*B*). However, neither route of MCA-MSC treatment affected basal epithelial thickness in Sal-treated control mice.

Subepithelial collagen deposition

Subepithelial collagen deposition was assessed morphometrically from Masson trichrome-stained lung sections and expressed as square micrometers per micrometer of BM length (Fig. 3). Subepithelial collagen deposition was significantly elevated in the Ova-injured mice (27.63 ± 0.66) compared with that in Sal-treated control mice (14.31 ± 1.87; $P < 0.001$ *vs.* Sal group) (Fig. 3*A*, *C*). Delivery of MCA-MSCs through IV injection modestly but significantly reduced the aberrant Ova-induced promotion of subepithelial collagen deposition (22.39 ± 1.78; $P < 0.05$ *vs.* Ova group; $P < 0.01$ *vs.* Sal group), whereas IN delivery of MCA-MSCs normalized the Ova-induced increase in subepithelial collagen deposition (16.98 ± 0.98; $P < 0.001$ *vs.* Ova group) back to that measured in Sal-treated control mice (not different from the Sal group) (Fig. 3*A*, *C*). As a result, the direct delivery of these MCA-MSCs into the lung of Ova-injured mice induced greater reversal of aberrant subepithelial collagen deposition compared with IV injection of these cells to Ova-injured mice ($P < 0.05$ *vs.* Ova MCA-MSC IV group) without affecting basal subepithelial collagen deposition when administered to Sal-treated control mice (Fig. 3*C*).

Total lung collagen concentration (fibrosis)

Total lung collagen concentration (% collagen concentration/dry weight lung tissue) was extrapolated from hydroxyproline levels present within the second largest lung lobe of each mouse and used as a measure of fibrosis (**Fig. 4**) and was significantly increased in Ova-injured mice (3.94 ± 0.09%) compared with that measured in Sal-treated control mice (2.89 ± 0.18%; $P < 0.001$ *vs.* Sal group). IV administration of MCA-MSCs to Ova-injured mice modestly but significantly reduced fibrosis in the lungs (3.62 ± 0.07%; $P < 0.05$ *vs.* Ova group; $P < 0.01$ *vs.* Sal group), whereas IN delivery of MCA-MSCs fully reversed aberrant lung collagen concentration levels back to those measured from Sal-treated mice (3.26 ± 0.17%; $P < 0.001$ *vs.* Ova group; not different from the Sal group) (Fig. 4). As observed with epithelial thickness (Fig. 3*B*) and subepithelial collagen thickness (Fig. 3*C*), direct (*i.e.*, IN) delivery of MCA-MSCs into the lung offered greater protection against the Ova-induced increase in total lung collagen concentration compared with the effects of IV delivery of these cells ($P < 0.01$ *vs.* Ova MCA-MSC IV group) without affecting basal collagen concentration levels when administered to Sal-treated control mice (Fig. 4).

Airway TGF-β1 expression

To determine the mechanisms by which MCA-MSCs were able to fully reverse Ova-induced subepithelial and total collagen deposition (fibrosis), the relative changes in airway TGF-β1 (profibrotic cytokine) expression levels were morphometrically assessed from IHC-stained lung sections and expressed as percentage staining per airway analyzed (**Fig. 5**). Airway TGF-β1 expression was significantly increased in Ova-injured mice (1.85 ± 0.13) compared with that measured in Sal-treated control mice (1.00 ± 0.08; $P < 0.001$ *vs.* Sal group) (Fig. 5). Both IV (1.06 ± 0.05) and IN (1.22 ± 0.05) delivery of MCA-MSCs to Ova-injured mice reversed aberrant airway TGF-β1 expression levels back to that measured in Sal-treated control mice (both $P < 0.001$ *vs.* Ova group; not different from Sal group) without affecting

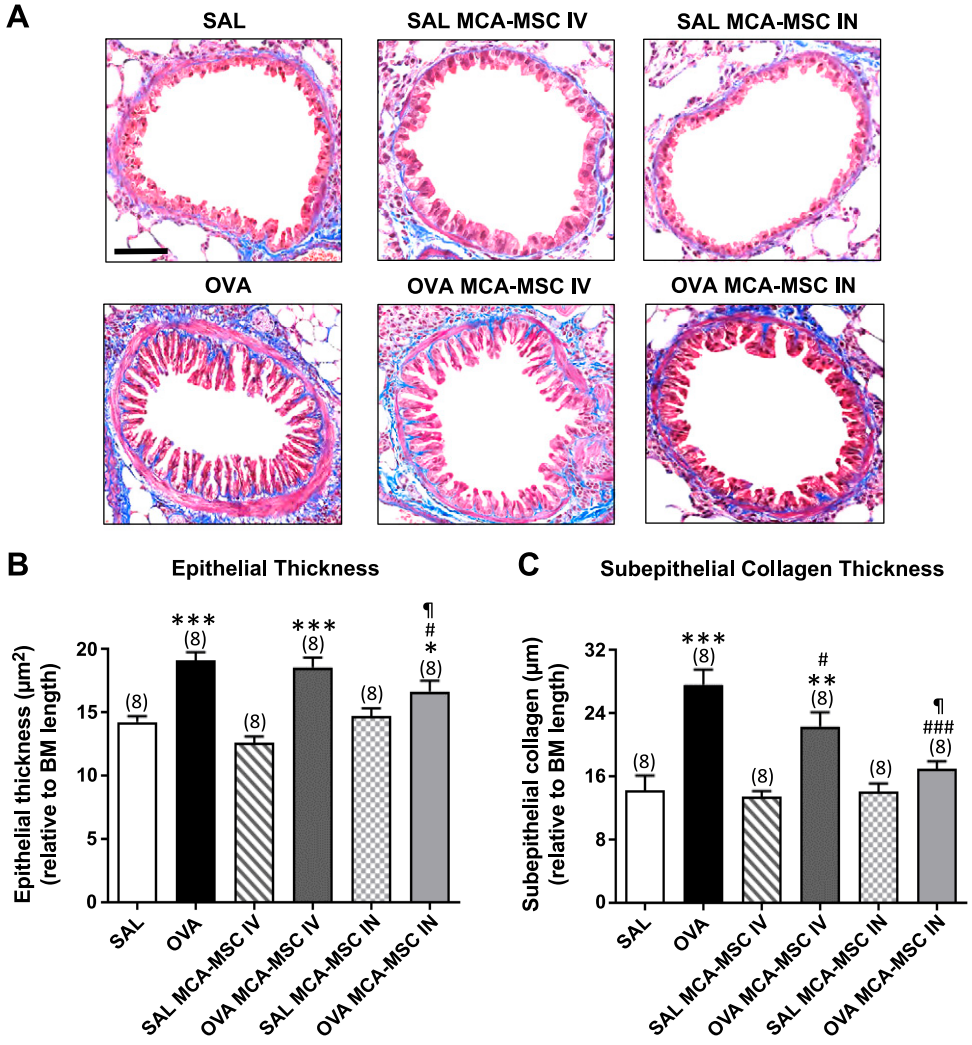

Figure 3. Effects of MCA-MSCs on airway epithelial thickness and subepithelial collagen deposition (fibrosis). *A*) Representative photomicrographs of Masson trichrome–stained lung sections from each of the groups studied show the extent of airway epithelial thickness and subepithelial collagen thickness (blue staining). Scale bar, 50 μm. Also shown is the mean ± SEM. *B, C*) Epithelial thickness (μm²) (*B*) and subepithelial collagen thickness (μm) (*C*) relative to BM length from 5 airways/mouse ($n = 8$ mice/group). $^{*}P < 0.05$, $^{**}P < 0.01$, $^{***}P < 0.001$ *vs.* Sal group; $^{\#}P < 0.05$, $^{\#\#\#}P < 0.001$ *vs.* Ova group; $^{\P}P < 0.05$ *vs.* Ova MCA-MSC IV group.

basal airway TGF-β1 expression levels when administered to Sal-treated control mice (Fig. 5).

Subepithelial myofibroblast density

Changes in α-SMA–stained subepithelial myofibroblast density were also morphometrically assessed from IHC-stained lung sections and expressed as the number of myofibroblasts per 100 μm of BM length (**Fig. 6**). Trace amounts of subepithelial α-SMA–positive myofibroblasts were detected in Sal-treated control mice (0.14 ± 0.05), whereas Ova-injured mice had an ~30-fold increase in myfibroblast density (4.37 ± 0.37; $P < 0.001$ *vs.* Sal group) (Fig. 6). IV administration of MCA-MSCs modestly but significantly reduced the Ova-induced increase in subepithelial myofibroblast density (3.42 ± 0.09; $P < 0.05$ *vs.* Ova group). In comparison, IN delivery of MCA-MSCs further reduced the Ova-induced promotion of subepithelial myofibroblast density (2.86 ± 0.27; $P < 0.001$ *vs.* Ova group) to a greater extent than IV administration of these cells ($P < 0.05$ *vs.* Ova MCA-MSC IV group) and in the absence of any effects on basal myofibroblast numbers when administered to Sal-treated control mice (Fig. 6). However, neither route of MCA-MSC administration fully reversed the aberrant subepithelial myofibroblast burden back to that measured in Sal-treated control mice (both $P < 0.001$ *vs.* Sal group) (Fig. 6).

Lung gelatinase expression

We also determined if the MCA-MSC–mediated reversal of Ova-induced airway/lung fibrosis was associated with their ability to influence collagen-degrading MMP levels. Gelatin zymography demonstrated that the lungs of female Balb/c mice predominantly expressed MMP-9 [gelatinase B; consistent with previous studies (15, 32)] and to a lesser extent MMP-13 (collagenase-3) (**Fig. 7**). Relative MMP-9 expression levels in Ova-injured mice (1.62 ± 0.22) were not significantly different from those measured in Sal-treated control animals (1.00 ± 0.09) (Fig. 7). In comparison, IV administration (3.77 ± 0.18), and to a greater extent IN administration (4.56 ± 0.20; $P < 0.05$ *vs.* Ova MCA-MSC IV group), of MCA-MSCs to Ova-injured mice markedly increased MMP-9 levels by ~1.3 and ~1.8-fold over what was measured in Ova-treated mice alone (both $P < 0.001$ *vs.* Ova group; $P < 0.001$ *vs.* Sal group) (Fig. 7). Interestingly, IV (1.95 ± 0.38) and IN (2.65 ± 0.30) delivery of MCA-MSCs to Sal-treated

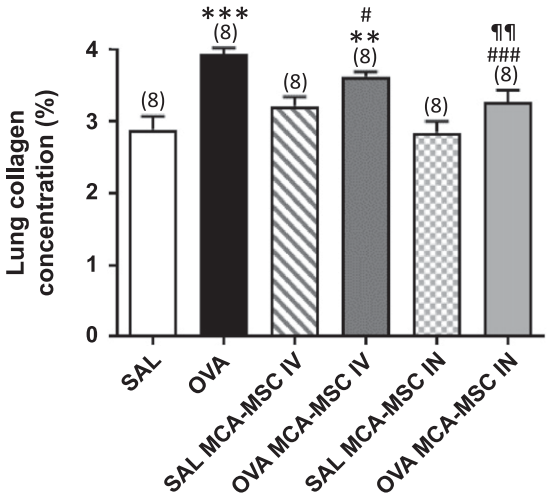

Figure 4. Effects of MCA-MSCs on total lung collagen concentration (another measure of fibrosis). Shown is the mean ± SEM total lung collagen concentration (% lung collagen content/dry weight tissue) from each of the groups studied measured from the second largest lung lobe per mouse (n = 8 mice/group). $^{**}P < 0.01$, $^{***}P < 0.001$ *vs.* Sal group; $^{\#}P < 0.05$, $^{\#\#\#}P < 0.001$ *vs.* Ova group; $^{\P}P < 0.05$ *vs.* Ova MCA-MSC IV group.

mice also significantly increased MMP-9 levels (both $P < 0.05$ *vs.* Sal group).

Effects of MCA-MSCs on AHR

AHR was assessed by invasive plethysmography in response to increasing concentrations of nebulized methacholine, which is a bronchoconstrictor (**Fig. 8**). Expectedly, Ova-treated mice had significantly elevated AHR compared with that measured in Sal-treated control mice ($P < 0.001$ *vs.* Sal group) (Fig. 8). IV delivery of MCA-MSCs partially (by ~50%) but significantly reversed the Ova-induced increase in AHR ($P < 0.05$ *vs.* Ova group), whereas IN administration of MCA-MSCs completely normalized the Ova-induced promotion of AHR ($P < 0.001$ *vs.* Ova group; $P < 0.01$ *vs.* Ova MCA-MSC IV group; not different from the Sal group) (Fig. 8). As with most other endpoints measured, neither route of MCS-MSC delivery affected basal AHR measurements when administered to Sal-treated control mice (Fig. 8).

DISCUSSION

This study assessed the therapeutic potential of novel iPSC-derived MCA-MSCs against the 3 central components of chronic AAD/asthma pathogenesis (AI, AWR, and AHR) when therapeutically administered intravenously or intranasally to established disease pathology. This represents the first study to assess such effects of MCA-derived MSCs in this *in vivo* setting because previous studies had evaluated the *in vivo* therapeutic effects of these cells in a hindlimb ischemic injury model (33). Both IV and IN administration of MCA-MSCs protected against the established AI, AWR (goblet cell metaplasia, aberrant airway TGF-β1 levels, subepithelial myofibroblast and collagen accumulation, total lung collagen concentration), and AHR that was induced by repeated Ova sensitization and challenge to mice (**Table 1**). However, the direct delivery of MCA-MSCs into the lungs of chronically allergic mice *via* the IN route was seen to offer greater protection against the Ova-induced increase in airway epithelial thickness and TGF-β1 levels, subepithelial myofibroblast and collagen accumulation, total lung collagen concentration, and AHR compared with IV delivery of these cells. This resulted in the complete reversal of aberrant airway

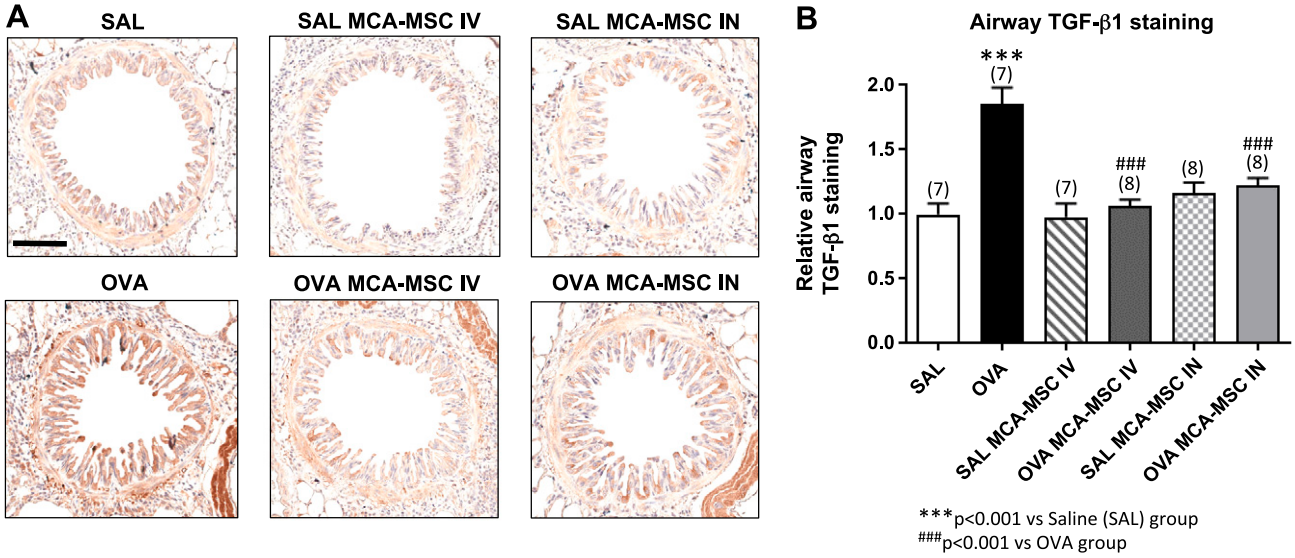

Figure 5. Effects of MCA-MSCs on airway TGF-β1 (profibrotic cytokine) expression. *A*) Representative photomicrographs of IHC-stained lung sections from each group studied show the extent of TGF-β1 staining and expression within and around the airway epithelial layer. Scale bar, 50 μm. *B*) Relative mean ± SEM TGF-β1 staining (%/field) from 5 airways/mouse (n = 7–8 mice/group). $^{***}P < 0.001$ *vs.* Sal group; $^{\#\#\#}P < 0.001$ *vs.* Ova group.

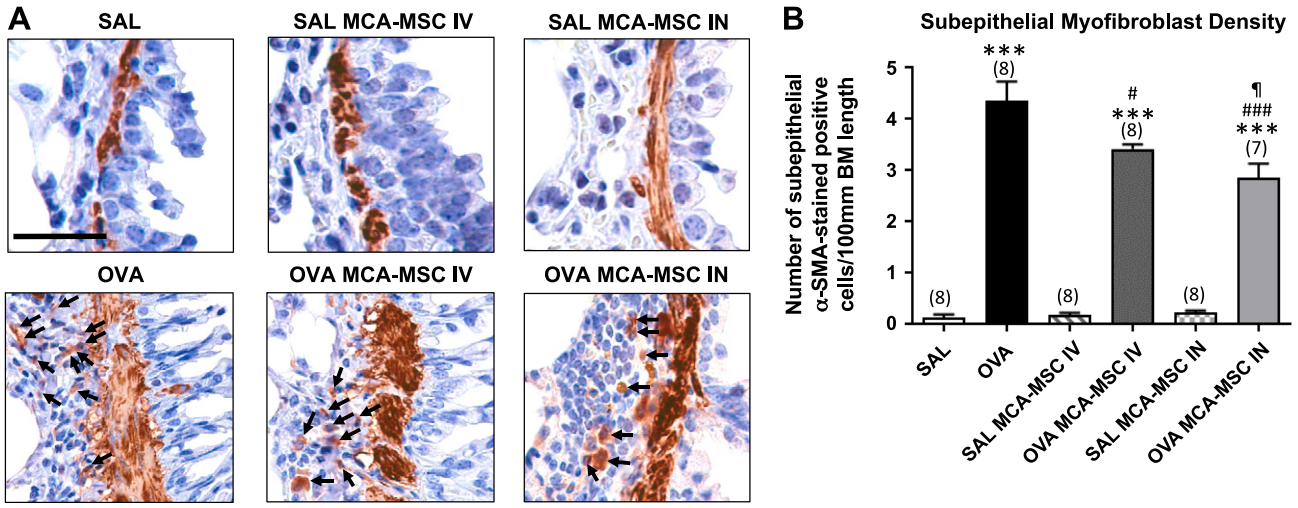

Figure 6. Effects of MCA-MSCs on subepithelial myofibroblast (key fibrosis-producing cell) density. *A*) Representative photomicrographs of IHC-stained lung sections from each group studied show the extent of α-SMA–stained myofibroblast density (as indicated by the arrows) within the airway subepithelial layer. Scale bar, 25 μm. *B*) Mean ± SEM number of myofibroblasts per 100 μm BM length from 5 airways/mouse (n = 7–8 mice/group). $^{***}P < 0.001$ *vs.* Sal group; $^{\#}P < 0.05$, $^{\#\#\#}P < 0.001$ *vs.* Ova group; $^{\P}P < 0.05$ *vs.* Ova MCA-MSC IV group.

TGF-β1 levels, airway/lung fibrosis, and AHR over a 2-wk (once weekly) treatment period and a significant increase collagen-degrading MMP-9 levels by IN delivery of MCA-MSCs (Table 1). Just as importantly, neither route of MCA-MSC administration was found to affect basal expression of the parameters measured, suggesting that IN delivery of MCA-MSC offers a safe and effective means of treating the central components of asthma.

The inflammatory component of asthma contributes to airway obstruction. The Th2-skewed inflammation results in the elevation of a particular subsets of cytokines, including IL-13, and the induction of goblet cell metaplasia (34). Consistent with our findings, previous studies have shown that IV injection of iPSC-MSCs could partially decrease the airway inflammatory score in an acute Ova model (35) by suppressing the levels of the Th2 cytokines, IL-4, IL-5, and IL-13. The systemic effects of MCA-MSCs may even be linked to their ability to activate regulatory T cells through direct cell-cell contact (17). Our current findings that MCA-MSCs, particularly when delivered intranasally to the allergic airways/lungs of mice, could markedly suppress AI (by ~75%) and goblet cell metaplasia (by ~50%) suggests that they mediate greater immunomodulatory properties compared with MSCs derived from the human bone marrow (15, 16) or adipose tissue (36). The direct administration of MCA-MSCs into the airways/lung would allow the protective factors they secrete to remain in the pulmonary environment. Furthermore, direct administration of MCA-MSCs allows the cells to remain in the inflamed lungs and hence have greater protective effects against allergen exposure mediated through the suppression of antigen-presenting cells, including alveolar macrophages (37) and dendritic cells (20).

Along with goblet cell metaplasia, epithelial proliferation is a major contributor to epithelial remodeling in asthma. Diminution in epithelial barrier function and desquamation culminate as epithelial proliferation (38). This proliferation is particularly extensive in severe asthma, where expansion of the epithelium leads to airway obstruction (39). Given that this reprogramming occurs early in the pathogenesis of asthma (40), asthma therapy should target the epithelium. When administered through IV injection, MCA-MSCs did not significantly affect the Ova-induced epithelial thickness. However, IN delivery of these cells resulted in a decreased epithelial thickness, despite both routes of delivery offering similar reductions in AI. This contrasts with previous findings related to bone marrow–derived MSCs in which the IN delivery of bone marrow MSCs alone had no effect on epithelial thickness (15). In that study, epithelial thickness was not affected by a decrease in AI. Hence, the difference observed between MCA-MSCs and bone marrow MSCs appears likely due to an active property of MCA-MSCs rather than being a passive effect produced by their ability to attenuate AI. Furthermore, in another study the administration of an epithelial factor repair peptide (trefoil factor-2) reduced epithelial thickness to the same extent as combination treatment with an antifibrotic and a corticosteroid, despite a greater decrease in AI offered by the combination treatment (41). As such, the reduction in epithelial proliferation was not mediated by a reduction in inflammation. With this additional evidence, the findings of our study may suggest either that the direct delivery of MCA-MSCs into the lung allows sufficient accumulation of paracrine factors that reduce epithelial thickness, or that these cells to come into direct contact with the damaged epithelium and mediate a reversal in its proliferation. This decrease in the epithelial thickness (and goblet cell metaplasia) provides the first piece of evidence of the ability of these MCA-derived MSCs to reverse AWR.

The culmination of a number of factors, including mechanical insults and allergens, can contribute to the destruction of the pulmonary architecture and airway function, leading to AWR in addition to AI. Damage due to

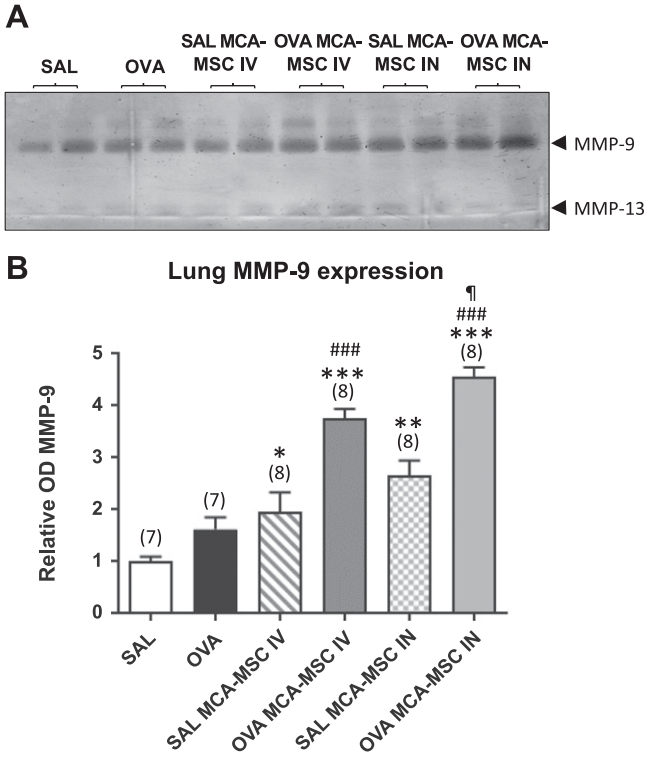

Figure 7. Effects of MCA-MSCs on MMP-9 (a collagen-degrading enzyme) levels. *A*) Representative gelatin zymograph (inverted image) showing the relative expression levels of lung MMP-9 (gelatinase B; 92 kDa) and MMP-13 (collagenase-3; ~55 kDa) in the each of the groups studied. In each case, 10 μg of total protein per sample were loaded onto zymographs for analysis, and separate zymographs analyzing 5 or 6 additional samples per group produced similar results. *B*) Relative mean ± SEM optical density MMP-9 (which is the most abundantly expressed gelatinase in the lung of female Balb/c mice) (n = 7–8 mice/group). $^{*}P < 0.05$, $^{**}P < 0.01$, $^{***}P < 0.001$ *vs.* Sal group; $^{\#\#\#}P < 0.001$ *vs.* Ova group; $^{\P}P < 0.05$ *vs.* Ova MCA-MSC IV group.

allergens or from heritable susceptibility causes the lungs to undergo endogenous processes of remodeling in an effort to self-repair structure and function of the airways, and these reparative processes result in aberrant wound healing, eventually leading to fibrosis (42, 43). Fibrosis was evident in the Ova-sensitized airways, which showed an elevation in aberrant subepithelial and total collagen levels. Although IV delivery of MCA-MSCs significantly reduced both aberrant subepithelial and total collagen deposition, IN delivery of these cells completely reversed this aberrant collagen deposition back to the levels seen in the uninjured saline-treated group. These results were unexpected because previous studies from our laboratory showed that the Ova-induced promotion of subepithelial and total collagen deposition could only be fully reversed when stem cell–based treatments were coadministered with serelaxin, an antifibrotic, hormone-based drug (15, 28), which similarly completely prevented fibrosis progression in a porcine model of myocardial infarction–induced heart failure (44) and in a murine model of tubulointerstitial renal disease (45). In these combination treatment studies (15, 44, 45), it was proposed that the antifibrotic effects of serelaxin (46) would create a more favorable environment in which stem cell–based therapies could be introduced, hence aiding stem cell survival and increasing their proliferative and migratory capacity to induce protective and therapeutic effects. Hence, IN delivery of MCA-MSCs could have similar effects to serelaxin or possess antifibrotic properties similar to fetal fibroblasts, which can facilitate wound healing in the absence of fibrosis (47). Further work is required to validate these hypotheses.

These results also correspond with the MCA-MSC–induced reduction in epithelial thickness observed. Fibrogenic growth factors are commonly released by epithelial cells in response to epithelial disturbances (48). In asthma this response is enhanced (49), suggesting that subepithelial fibrosis results from a conduit of signals from a defective epithelium to the deeper airway wall. As such, MCA-MSCs could exert their antifibrotic effects *via* immunomodulatory properties and possible secretion of antifibrotic mediators given the reduction in subepithelial and total collagen when administered intravenously. The further reduction seen when these cells were given intranasally may be caused by their ability to reduce epithelial thickness, which likely reduces epithelial disturbances and production of fibrogenic growth factors.

The key finding of this study was that MCA-MSCs, when given intranasally, reversed fibrosis and reverted AHR to levels measured in uninjured mice. These findings are consistent with previous studies that show that therapies that were able to abrogate AWR, specifically aberrant airway collagen deposition and TGF-β1 levels, were seen to reverse AHR (15, 28, 32, 41). AHR is driven by airway obstruction, which can be caused by mucus

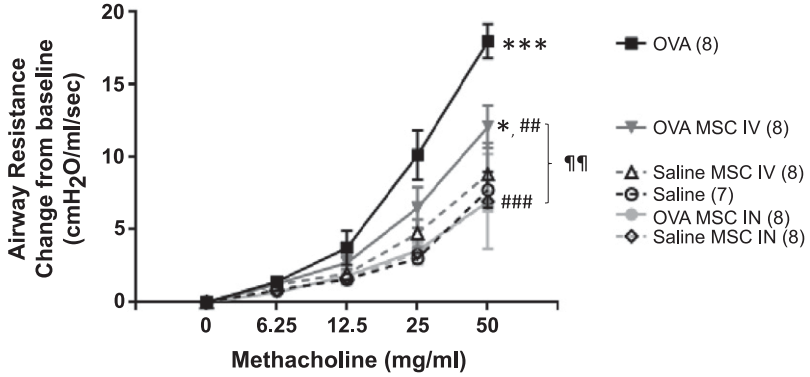

Figure 8. Effects of MCA-MSCs on AHR. Airway resistance (reflecting changes in AHR) was assessed *via* invasive plethysmography in response to increasing doses of nebulized methacholine (a bronchoconstrictor. Results are expressed as resistance change from baseline. Shown is the mean ± SEM airway resistance to each dose of methacholine tested (n = 7–8 mice/group). $^{*}P < 0.05$, $^{***}P < 0.001$ *vs.* Sal group; $^{\#\#}P < 0.01$, $^{\#\#\#}P < 0.001$ *vs.* Ova group; $^{\P\P}P < 0.01$ *vs.* Ova MCA-MSC IV group.

TABLE 1. *Summary of the effects of MCA-MSCs on the pathologies of chronic AAD*

Key feature of human asthma	Ova	Sal MCA-MSC IV	Ova MCA-MSC IV	Sal MCA-MSC IN	Ova MCA-MSC IN
AI	↑↑↑	–	↓	–	↓↓
Goblet cell metaplasia	↑↑↑	–	↓	–	↓↓
Epithelial thickness	↑↑↑	–	–	–	↓↓*
Subepithelial collagen	↑↑↑	–	↓	–	↓↓↓*
Total lung collagen	↑↑↑	–	↓	–	↓↓↓*
Airway TGF-β1 levels	↑↑↑	–	↓↓↓	–	↓↓↓
Subepithelial myofibroblast density	↑↑↑	–	↓	–	↓↓*
Lung MMP-9 levels	–	↑	↑↑↑	↑↑	↑↑↑*
AHR	↑↑↑	–	↓↓	–	↓↓↓**

The arrows in the Ova, Sal MCA-MSC IV, and Sal MCA-MSC IN columns are reflective of changes to that measured in Sal-treated mice, whereas the arrows in the Ova MCA-MSC IV and Ova MCA-MSC IN columns are reflective of changes to that in the Ova alone group. Dashes indicate no change compared with Sal or Ova-treated mice. $*P < 0.05$, $**P < 0.01$ *vs.* Ova MCA-MSC IV group.

plugging from goblet cell metaplasia (50) and by epithelial thickening (38). In addition, the interaction between AI and fibrosis of the airway wall leads to an environment that elevates AHR. Not only does fibrosis decrease airway compliance in patients with asthma (51), but this expansion in ECM leads to the retention of soluble inflammatory mediators and the chronic persistence of established AHR (52). As such, AHR could be reverted to normal uninjured levels mainly by the reduction of subepithelial fibrosis and attenuation of AI afforded by MCA-MSCs but could also be caused by a decrease in airway obstruction mediated by the reduced counts of goblet cells and lower levels of epithelial thickening. In our study, it is likely that these MCA-MSCs corrected AHR by targeting AWR at a number of levels, in addition to their anti-inflammatory effects.

In summary, the present study, the first on MCA-MSCs in chronic AAD, found that MCA-MSCs could effectively reduce AI and reverse markers of AWR as well as AHR. Therefore, MCA-MSCs may provide a novel stand-alone therapy or an adjunct therapy for subpopulations of asthma sufferers who do not respond to current (corticosteroid) therapy. Furthermore, IN delivery of these cells was found to be more effective in eliciting therapeutic benefits compared with IV delivery, with maximal benefits demonstrated against airway fibrosis and AHR when directly delivered to the allergic airways/lungs. A striking finding that separates these MCA-MSCs from other stem cells previously studied is that other MSCs/stem cells only produced similar effects to MCA-MSCs when applied in combination with other therapies (15, 28). Future studies comparing and combining the effects of these MCA-MSCs with current asthma medications and aimed at understanding their mode of actions are needed. FJ

ACKNOWLEDGMENTS

The authors acknowledge the facilities and technical assistance of Monash Histology Platform (Department of Anatomy and Developmental Biology, Monash University). This work was supported by a National Health and Medical Research Council (NHMRC) of Australia Senior Research Fellowship (GNT1041766) to C.S.S., and by Cynata Therapeutics funding to C.S.S. and S.G.R. S.G.R., S.R., B.R.S.B., and C.S.S. are with the Cardiovascular Disease Program, Biomedicine Discovery Institute and Department of Pharmacology, Monash University. S.G.R. is also affiliated with the Central Clinical School, Monash University. K.K. is an employee and shareholder of Cynata Therapeutics Ltd., but was not involved with performing the experiments or analysis of data.

AUTHOR CONTRIBUTIONS

S. G. Royce and C. S. Samuel designed the research; S. G. Royce, S. Rele, B. R. S. Broughton, and C. S. Samuel performed research; K. Kelly contributed new reagents; S. G. Royce, S. Rele, and C. S. Samuel analyzed the data; and S. G. Royce, S. Rele, B. R. S. Broughton, K. Kelly, and C. S. Samuel wrote the paper.

REFERENCES

1. Braman, S. S. (2006) The global burden of asthma. *Chest* **130** (1 Suppl), 4S–12S
2. Holgate, S. T., Arshad, H. S., Roberts, G. C., Howarth, P. H., Thurner, P., and Davies, D. E. (2009) A new look at the pathogenesis of asthma. *Clin. Sci. (Lond)* **118**, 439–450
3. Royce, S. G., Moodley, Y., and Samuel, C. S. (2014) Novel therapeutic strategies for lung disorders associated with airway remodelling and fibrosis. *Pharmacol. Ther.* **141**, 250–260
4. Nelson, H. S., Weiss, S. T., Bleecker, E. R., Yancey, S. W., and Dorinsky, P. M.; SMART Study Group. (2006) The salmeterol multicenter asthma research trial: a comparison of usual pharmacotherapy for asthma or usual pharmacotherapy plus salmeterol. *Chest* **129**, 15–26
5. Cates, C. J., Jaeschke, R., Schmidt, S., and Ferrer, M. (2013) Regular treatment with salmeterol and inhaled steroids for chronic asthma: serious adverse events. *Cochrane Database Syst. Rev.* **3**, CD006922
6. Cates, C. J., Jaeschke, R., Schmidt, S., and Ferrer, M. (2013) Regular treatment with formoterol and inhaled steroids for chronic asthma: serious adverse events. *Cochrane Database Syst. Rev.* **6**, CD006924
7. Wener, R. R., and Bel, E. H. (2013) Severe refractory asthma: an update. *Eur. Respir. Rev.* **22**, 227–235
8. Reddel, H. K., Jenkins, C. R., Marks, G. B., Ware, S. I., Xuan, W., Salome, C. M., Badcock, C. A., and Woolcock, A. J. (2000) Optimal asthma control, starting with high doses of inhaled budesonide. *Eur. Respir. J.* **16**, 226–235
9. Adams, N. P., Bestall, J. C., Jones, P., Lasserson, T. J., Griffiths, B., and Cates, C. J. (2008) Fluticasone at different doses for chronic asthma in adults and children. *Cochrane Database Syst. Rev.* **4**, CD003534
10. Knight, D. A., Rossi, F. M., and Hackett, T. L. (2010) Mesenchymal stem cells for repair of the airway epithelium in asthma. *Expert Rev. Respir. Med.* **4**, 747–758
11. Sueblinvong, V., and Weiss, D. J. (2010) Stem cells and cell therapy approaches in lung biology and diseases. *Transl. Res.* **156**, 188–205
12. Abreu, S. C., Antunes, M. A., Maron-Gutierrez, T., Cruz, F. F., Ornellas, D. S., Silva, A. L., Diaz, B. L., Ab'Saber, A. M., Capelozzi, V. L., Xisto, D. G., Morales, M. M., and Rocco, P. R. (2013) Bone

marrow mononuclear cell therapy in experimental allergic asthma: intratracheal versus intravenous administration. *Respir. Physiol. Neurobiol.* **185**, 615–624
13. Martínez-González, I., Cruz, M. J., Moreno, R., Morell, F., Muñoz, X., and Aran, J. M. (2014) Human mesenchymal stem cells resolve airway inflammation, hyperreactivity, and histopathology in a mouse model of occupational asthma. *Stem Cells Dev.* **23**, 2352–2363
14. Inamdar, A. C., and Inamdar, A. A. (2013) Mesenchymal stem cell therapy in lung disorders: pathogenesis of lung diseases and mechanism of action of mesenchymal stem cell. *Exp. Lung Res.* **39**, 315–327
15. Royce, S. G., Shen, M., Patel, K. P., Huuskes, B. M., Ricardo, S. D., and Samuel, C. S. (2015) Mesenchymal stem cells and serelaxin synergistically abrogate established airway fibrosis in an experimental model of chronic allergic airways disease. *Stem Cell Res. (Amst.)* **15**, 495–505
16. Urbanek, K., De Angelis, A., Spaziano, G., Piegari, E., Matteis, M., Cappetta, D., Esposito, G., Russo, R., Tartaglione, G., De Palma, R., Rossi, F., and D'Agostino, B. (2016) Intratracheal administration of mesenchymal stem cells modulates tachykinin system, suppresses airway remodeling and reduces airway hyperresponsiveness in an animal model. *PLoS One* **11**, e0158746
17. Gao, F., Chiu, S. M., Motan, D. A., Zhang, Z., Chen, L., Ji, H. L., Tse, H. F., Fu, Q. L., and Lian, Q. (2016) Mesenchymal stem cells and immunomodulation: current status and future prospects. *Cell Death Dis.* **7**, e2062
18. Goodwin, M., Sueblinvong, V., Eisenhauer, P., Ziats, N. P., LeClair, L., Poynter, M. E., Steele, C., Rincon, M., and Weiss, D. J. (2011) Bone marrow-derived mesenchymal stromal cells inhibit Th2-mediated allergic airways inflammation in mice. *Stem Cells* **29**, 1137–1148
19. Ou-Yang, H. F., Huang, Y., Hu, X. B., and Wu, C. G. (2011) Suppression of allergic airway inflammation in a mouse model of asthma by exogenous mesenchymal stem cells. *Exp. Biol. Med. (Maywood)* **236**, 1461–1467
20. Zeng, S. L., Wang, L. H., Li, P., Wang, W., and Yang, J. (2015) Mesenchymal stem cells abrogate experimental asthma by altering dendritic cell function. *Mol. Med. Rep.* **12**, 2511–2520
21. Ogulur, I., Gurhan, G., Aksoy, A., Duruksu, G., Inci, C., Filinte, D., Kombak, F. E., Karaoz, E., and Akkoc, T. (2014) Suppressive effect of compact bone-derived mesenchymal stem cells on chronic airway remodeling in murine model of asthma. *Int. Immunopharmacol.* **20**, 101–109
22. Lim, R., Milton, P., Murphy, S. V., Dickinson, H., Chan, S. T., and Jenkin, G. (2013) Human mesenchymal stem cells reduce lung injury in immunocompromised mice but not in immunocompetent mice. *Respiration* **85**, 332–341
23. Kapoor, S., Patel, S. A., Kartan, S., Axelrod, D., Capitle, E., and Rameshwar, P. (2012) Tolerance-like mediated suppression by mesenchymal stem cells in patients with dust mite allergy-induced asthma. *J. Allergy Clin. Immunol.* **129**, 1094–1101
24. Mancheño-Corvo, P., Menta, R., del Río, B., Franquesa, M., Ramírez, C., Hoogduijn, M. J., DelaRosa, O., Dalemans, W., and Lombardo, E. (2015) T lymphocyte prestimulation impairs in a time-dependent manner the capacity of adipose mesenchymal stem cells to inhibit proliferation: role of interferon γ, poly I:C, and tryptophan metabolism in restoring adipose mesenchymal stem cell inhibitory effect. *Stem Cells Dev.* **24**, 2158–2170
25. Weiss, D. J. (2014) Concise review: current status of stem cells and regenerative medicine in lung biology and diseases. *Stem Cells* **32**, 16–25
26. Vodyanik, M. A., Yu, J., Zhang, X., Tian, S., Stewart, R., Thomson, J. A., and Slukvin, I. I. (2010) A mesoderm-derived precursor for mesenchymal stem and endothelial cells. *Cell Stem Cell* **7**, 718–729
27. Royce, S. G., Sedjahtera, A., Samuel, C. S., and Tang, M. L. (2013) Combination therapy with relaxin and methylprednisolone augments the effects of either treatment alone in inhibiting subepithelial fibrosis in an experimental model of allergic airways disease. *Clin. Sci.* **124**, 41–51
28. Royce, S. G., Tominaga, A. M., Shen, M., Patel, K. P., Huuskes, B. M., Lim, R., Ricardo, S. D., and Samuel, C. S. (2016) Serelaxin improves the therapeutic efficacy of RXFP1-expressing human amnion epithelial cells in experimental allergic airway disease. *Clin. Sci.* **130**, 2151–2165
29. Dominici, M., Le Blanc, K., Mueller, I., Slaper-Cortenbach, I., Marini, F., Krause, D., Deans, R., Keating, A., Prockop, Dj., and Horwitz, E. (2006) Minimal criteria for defining multipotent mesenchymal stromal cells. The International Society for Cellular Therapy position statement. *Cytotherapy* **8**, 315–317
30. Gallop, P. M., and Paz, M. A. (1975) Posttranslational protein modifications, with special attention to collagen and elastin. *Physiol. Rev.* **55**, 418–487
31. Woessner, J. F., Jr. (1995) Quantification of matrix metalloproteinases in tissue samples. *Methods Enzymol.* **248**, 510–528
32. Royce, S. G., Lim, C., Muljadi, R. C., Samuel, C. S., Ververis, K., Karagiannis, T. C., Giraud, A. S., and Tang, M. L. (2013) Trefoil factor-2 reverses airway remodeling changes in allergic airways disease. *Am. J. Respir. Cell Mol. Biol.* **48**, 135–144
33. Koch, J. M., D'Souza, S. S., Schwahn, D. J., Dixon, I., and Hacker, T. A. (2016) Mesenchymoangioblast-derived mesenchymal stromal cells inhibit cell damage, tissue damage and improve peripheral blood flow following hindlimb ischemic injury in mice. *Cytotherapy* **18**, 219–228
34. Cohn, L., Elias, J. A., and Chupp, G. L. (2004) Asthma: mechanisms of disease persistence and progression. *Annu. Rev. Immunol.* **22**, 789–815
35. Sun, Y. Q., Deng, M. X., He, J., Zeng, Q. X., Wen, W., Wong, D. S., Tse, H. F., Xu, G., Lian, Q., Shi, J., and Fu, Q. L. (2012) Human pluripotent stem cell-derived mesenchymal stem cells prevent allergic airway inflammation in mice. *Stem Cells* **30**, 2692–2699
36. Cho, K. S., Park, M. K., Mun, S. J., Park, H. Y., Yu, H. S., and Roh, H. J. (2016) Indoleamine 2,3-Dioxygenase is not a pivotal regulator responsible for suppressing allergic airway inflammation through adipose-derived stem cells. *PLoS One* **11**, e0165661
37. Mathias, L. J., Khong, S. M., Spyroglou, L., Payne, N. L., Siatskas, C., Thorburn, A. N., Boyd, R. L., and Heng, T. S. (2013) Alveolar macrophages are critical for the inhibition of allergic asthma by mesenchymal stromal cells. *J. Immunol.* **191**, 5914–5924
38. Shifren, A., Witt, C., Christie, C., and Castro, M. (2012) Mechanisms of remodeling in asthmatic airways. *J. Allergy (Cairo)* **2012**, 316049
39. Cohen, L., E, X., Tarsi, J., Ramkumar, T., Horiuchi, T. K., Cochran, R., DeMartino, S., Schechtman, K. B., Hussain, I., Holtzman, M. J., and Castro, M.; NHLBI Severe Asthma Research Program (SARP). (2007) Epithelial cell proliferation contributes to airway remodeling in severe asthma. *Am. J. Respir. Crit. Care Med.* **176**, 138–145
40. Carsin, A., Mazenq, J., Ilstad, A., Dubus, J. C., Chanez, P., and Gras, D. (2016) Bronchial epithelium in children: a key player in asthma. *Eur. Respir. Rev.* **25**, 158–169
41. Patel, K. P., Giraud, A. S., Samuel, C. S., and Royce, S. G. (2016) Combining an epithelial repair factor and anti-fibrotic with a corticosteroid offers optimal treatment for allergic airways disease. *Br. J. Pharmacol.* **173**, 2016–2029
42. Holgate, S. T. (2008) Pathogenesis of asthma. *Clin. Exp. Allergy* **38**, 872–897
43. Holgate, S. T., and Davies, D. E. (2009) Rethinking the pathogenesis of asthma. *Immunity* **31**, 362–367
44. Formigli, L., Perna, A. M., Meacci, E., Cinci, L., Margheri, M., Nistri, S., Tani, A., Silvertown, J., Orlandini, G., Porciani, C., Zecchi-Orlandini, S., Medin, J., and Bani, D. (2007) Paracrine effects of transplanted myoblasts and relaxin on post-infarction heart remodelling. *J. Cell. Mol. Med.* **11**, 1087–1100
45. Huuskes, B. M., Wise, A. F., Cox, A. J., Lim, E. X., Payne, N. L., Kelly, D. J., Samuel, C. S., and Ricardo, S. D. (2015) Combination therapy of mesenchymal stem cells and serelaxin effectively attenuates renal fibrosis in obstructive nephropathy. *FASEB J.* **29**, 540–553
46. Samuel, C. S., Summers, R. J., and Hewitson, T. D. (2016) Antifibrotic actions of serelaxin - new roles for an old player. *Trends Pharmacol. Sci.* **37**, 485–497
47. Rolfe, K. J., and Grobbelaar, A. O. (2012) A review of fetal scarless healing. *ISRN Dermatol.* **2012**, 698034
48. Holgate, S. T. (2000) Epithelial damage and response. *Clin. Exp. Allergy* **30** (Suppl 1), 37–41
49. Hastie, A. T., Kraft, W. K., Nyce, K. B., Zangrilli, J. G., Musani, A. I., Fish, J. E., and Peters, S. P. (2002) Asthmatic epithelial cell proliferation and stimulation of collagen production: human asthmatic epithelial cells stimulate collagen type III production by human lung myofibroblasts after segmental allergen challenge. *Am. J. Respir. Crit. Care Med.* **165**, 266–272
50. Curran, D. R., and Cohn, L. (2010) Advances in mucous cell metaplasia: a plug for mucus as a therapeutic focus in chronic airway disease. *Am. J. Respir. Cell Mol. Biol.* **42**, 268–275
51. Broide, D. H. (2008) Immunologic and inflammatory mechanisms that drive asthma progression to remodeling. *J. Allergy Clin. Immunol.* 121, 560–570; quiz 571–562
52. Pitchford, S., and Page, C. (2003) Extracellular matrix composition influences the resistance of airway remodelling events towards glucocorticoid treatment. *Br. J. Pharmacol.* **138**, 1181–1182

Received for publication February 27, 2017.
Accepted for publication May 22, 2017.